Single-cell analysis of the CD8$^+$ T-cell compartment in multiple myeloma reveals disease specific changes are chiefly restricted to a CD69$^-$ subset suggesting potent cytotoxic effectors exist within the tumor bed

James Favaloro,[1,2*] Christian E. Bryant,[1,3*] Edward Abadir,[1,3] Samuel Gardiner,[4] Shihong Yang,[1] Tracy King,[1,3] Najah Nassif,[2] Lisa M. Sedger,[5,6] Richard Boyle,[7] Douglas E. Joshua[1,3] and P. Joy Ho[1,2,3]

[1]Institute of Hematology, Multiple Myeloma Research Laboratory, New South Wales Health Pathology, Royal Prince Alfred Hospital, Camperdown; [2]School of Life Sciences, University of Technology Sydney, Ultimo, Sydney; [3]Sydney Medical School, the University of Sydney, Sydney; [4]Sydney Local Health District Clinical Research Institute, Royal Prince Alfred Hospital, Camperdown; [5]Institute for Clinical Pathology and Medical Research (ICPMR), New South Wales Health Pathology, Westmead Hospital, Westemead; [6]Center for Virus Research, Westmead Institute for Medical Research, Westmead and New South Wales, Sydney and [7]Orthopedics Department, Sydney Local Health District, Royal Prince Alfred Hospital, Camperdown, New South Wales, Australia

JF and CEB contributed equally as first authors.

Correspondence: J. Favaloro
james.favaloro@health.nsw.gov.au

C.E. Bryant
christian.bryant@health.nsw.gov.au.

Received: May 14, 2023.
Accepted: September 28, 2023.
Early view: October 5, 2023.

https://doi.org/10.3324/haematol.2023.283062

Abstract

Multiple myeloma (MM) is an incurable disease of the bone marrow (BM) characterized by the uncontrolled proliferation of neoplastic plasma cells. While CD8$^+$ T cells have an established role in disease control, few studies have focused on these cells within the MM tumor microenvironment (TME). We analyzed CD8$^+$ T cells in the BM and peripheral blood (PB) of untreated patients with MM and non-myeloma controls using flow cytometry, mass cytometry and single-cell RNA sequencing, using several novel bioinformatics workflows. Inter-tissue differences were most evident in the differential expression of Granzymes B and K, which were strongly associated with two distinct subsets of CD8$^+$ T cells delineated by the expression of CD69, accounting for roughly 50% of BM-CD8$^+$ T cells of all assessed cohorts. While few differences were observable between health and disease in the BM-restricted CD8CD69$^+$ T-cell subset, the CD8$^+$CD69$^-$ T-cell subset in the BM of untreated MM patients demonstrated increased representation of highly differentiated effector cells and evident compositional parallels between the PB, absent in age-matched controls, where a marked reduction of effector cells was observed. We demonstrate the transcriptional signature of BM-CD8$^+$ T cells from patients with MM more closely resembles TCR-activated CD8$^+$ T cells from age-matched controls than their resting counterparts.

Introduction

Multiple myeloma (MM) is an incurable disease of the bone marrow (BM). It is preceded by the premalignant stage monoclonal gammopathy of undetermined significance (MGUS) and is characterized by the uncontrolled proliferation of neoplastic plasma cells (PC).[1] Healthy BM is a heterogeneous tissue that is highly vascularized and the site of hematopoiesis.[2] The BM acts as a reservoir of antigen-experienced CD8$^+$ tissue-resident memory T cells (T_{RM})[3] and long-lived PC.[4] MM has an established detrimental effect on this compartment,[5] as the BM transforms to an increasingly hypoxic, inflammatory, myeloma-promotive tumor microenvironment (TME), non-conducive to normal homeostasis.[6]

Substantial evidence exists to support the concept that CD8$^+$ T cells play an important role in disease control.[7] We have previously shown that T-cell receptor (TCR) Vβ restricted terminally differentiated CD8$^+$ T-cell (T_{TE}) clonal expansions are detectable in the peripheral blood (PB) of

patients with MM and their presence correlates with improved patient outcomes.[8] These cells have a senescent secretory effector phenotype,[9] including low levels of programmed cell death protein 1 (PD-1), which may in part explain the poor results with anti-PD-1 monotherapy.[10] T cells circulate between the BM and PB, and in MM, cells entering the TME are exposed to myeloma-associated antigens.[11] Recently, we demonstrated that clonally expanded TCRVβ restricted CD8+ T_{TE}, capable of exerting specific killing of autologous MM cells *in vitro*, are detectable in the BM of several patients.[12] Despite this, the effect of the TME on these crucial effectors, as well as the plethora of other CD8+ T-cell subsets has not been investigated in-depth. Thus, a comprehensive analysis of CD8+ T cells in the BM and PB of patients with MM may permit a greater understanding of disease and the host immune response. In this study, we analyzed CD8+ T cells in the BM and PB of age-matched controls, premalignant MGUS, and untreated, newly diagnosed (ND) patients with MM using flow cytometry, mass cytometry and single-cell RNA sequencing (scRNA-Seq). We show that CD8+ T cells from the BM of all subjects can be divided based on the expression of CD69 and these cells demonstrate unique, disease-associated Granzyme expression patterns. We further show the transcriptional signature of BM-CD8+ T cells from patients with MM resemble TCR-activated CD8+ T cells from age-matched controls.

Methods

Patients and controls

MGUS and NDMM patients, diagnosed by the International Myeloma Working Group criteria, were recruited through the Department of Hematology, Royal Prince Alfred Hospital (RPAH). Age-matched controls without diagnosed malignancy or active infection, undergoing hip arthroplasty were recruited through the Department of Orthopedic Surgery, RPAH. Characteristics of patients and controls are summarized in Table 1. Paired BM and PB samples were collected and analyzed by mass cytometry, flow cytometry or scRNA-seq. The study was approved by the Institutional Human Research Ethics Committee. All patients provided informed consent before sample collection, following the amended Declaration of Helsinki.

Single-cell RNA/T-cell receptor sequencing

Purified CD8+ cells were isolated from cryopreserved samples through a two-stage enrichment using a human CD8+ T-cell Isolation kit (Miltenyi Biotech) followed by FACS sorting as $CD45^+CD8^+CD4^-CD56^-$ cells on a BD FACS Aria II. Single cells were encapsulated for cDNA synthesis and barcoded using the Chromium Single-cell 5′ V(D)J Reagent kit v1.1 (10x Genomics) followed by library construction according to the manufacturer's recommendations. Libraries were sequenced on an Illumina NovaSeq 6000 (NovaSeq Control

Table 1. General and clinical characteristics of patients and controls.

Characteristics	NDMM N=21	MGUS N=3	Controls N=12
Age in years, median (range)	72 (48-90)	62 (56-65)	66 (57-83)
Sex: male, N (%)	14 (66)	1 (33)	4 (25)
R-ISS stage, N (%) R-ISS 1 R-ISS 2 R-ISS 3	 4 (19) 14 (67) 3 (14)	 N/A N/A N/A	 N/A N/A N/A
Isotype, N (%) IgG IgA Light chain	 13 (62) 5 (24) 3 (14)	 N/A N/A N/A	 N/A N/A N/A
Cytogenetics, N (%) 17p deletion −1p and/or +1q	19 (90) 1 (5) 9 (47)	N/A N/A N/A	N/A N/A N/A
FISH, N (%) t(4;14) t(14;16) del17p	21 (100) 3 (14) 0 (0) 0 (0)	N/A N/A N/A N/A	N/A N/A N/A N/A
LDH U/L median (range) Above normal, N (%)	155 (84-279) 1 (5)	N/A N/A	N/A N/A

NDMM: newly diagnosed multiple myeloma; MGUS: monoclonal gammopathy of undetermined significance; FISH: fluorescence *in situ* hybridization; IgA: immunoglobulin A; IgG: immunoglobulin G; R-ISS: Revised International Staging System; LDH: lactate dehydrogenase; N/A: not applicable.

Software v.1.6.0 / Real-Time Analysis v.3.4.4) using a NovaSeq S4 reagent kit (Illumina). Bioinformatics analysis is detailed in the *Online Supplementary Appendix*.

Flow and mass cytometry

Flow cytometry was performed with monoclonal antibodies (mAb) targeting surface antigens (*Online Supplementary Table S1*), fixed and permeabilized using either fixation/permeabilization buffer (BD Biosciences) for assessment of intracellular cytokines or Foxp3/Transcription Factor Staining Buffer Set (Thermo-Fisher Scientific) for assessment of transcription factors, then stained with mAb specific to intracellular proteins Granzyme B, Granzyme K and Perforin in perm/wash buffer (BD Biosciences) or TCF-1 in permeabilization buffer (Thermo-Fisher Scientific). Analysis of flow cytometry data was performed using FlowJo (Version 10.8.1, BD Biosciences). Mass cytometry utilized an expanded panel of antibodies (*Online Supplementary Table S2*) and is detailed in the *Online Supplementary Appendix*. Gating of T-cell subsets followed our previously defined approach (*Online Supplementary Figure S1*).

Statistical analysis

The non-parametric Mann-Whitney U and the Wilcoxon Signed Rank test were used to compare unpaired and paired data sets respectively. Statistical significance was determined at $P<0.05$ for all statistical analyses and was performed using GraphPad Prism version 9.01 (GraphPad Software) or R (v. 4.2.1 [see *Online Supplementary Appendix*]).

Results

Unsupervised clustering reveals an unequal distribution of memory, effector and naïve-like subsets in the bone marrow and peripheral blood of newly diagnosed multiple myeloma patients

Although CD8+ T cells are well documented to contribute to disease control in MM,[7] the effect of the TME on these cells is poorly understood. We constructed a transcriptomic map of CD8+ T cells purified from the BM and PB of newly diagnosed multiple myeloma (NDMM) patients using the 10x genomics platform (*Online Supplementary Figure S2A*). After strict quality control (QC), we recovered transcriptional data from an average of 6,929 cells from paired BM and PB samples and an average of 1,146 genes and 3,317 unique molecular identifiers (*Online Supplementary Table S3*).

Unsupervised clustering in an integrated analysis revealed six clusters (Figure 1Ai), with broad differences between BM and PB samples observable on Uniform Manifold Approximation and Projection (UMAP), with PB cells containing a more prominent terminal effector population than those from BM (Figure 1Aii). Canonical transcriptional signatures, assisted by the cell type identification R package "SingleR", in conjunction with reference datasets, permitted annotation of clusters (Figure 1B; *Online Supplementary Table S4*). The dominant cluster was representative of activated and/or stressed CD8+ effector memory T cells (T_{EM}), defined by the expression *GZMK*, several AP-1 associated genes: *DUSP2*, *JUN*, *DUSP1*, *JUNB* and *FOS*, and activation markers *CD69* and *CD74*, in addition to reduced expression of genes associated with naïve T cells (T_N) and central memory T cells (T_{CM}) (i.e., *SELL*, *LTB*, *CCR7* and *IL7R*). The second most dominant cluster, representative of CD8+ T_{TE} was characterized by genes associated primarily with cytotoxicity: *GNLY*, *GZMB*, *NKG7*, *PRF1* and *LGALS1*, in addition to reduced expression of genes that defined both the dominant T_{EM} cluster and smaller T_N and T_{CM} clusters. The T_N cluster was identified by genes associated with cell homing, metabolism and stemness: *SELL*, *LTB*, *CCR7*, and *TCF7* and reduced expression of genes associated with T_{EM} and T_{TE}. Beyond the three major clusters, three smaller clusters were identified: (i) the first comprising a mixture of cytotoxic cells characterized by expression of *GZMA*, *KLRB1* and *KLRD1* and reduced expression of naïve-associated genes was designated as a cytotoxic memory cluster (Cyto-T_{EM}); (ii) a small cluster characterized by higher than average levels of five genes associated with chemotaxis: *CCL4*, *CCL3*, *CCL4L2*, *XCL2* and *XCL1* shares features of recently defined pre-exhausted T cells (P_{RE}-EX);[13] (iii) the smallest cluster shared many features with T_N, additionally expressed high levels of *IL7R* and *LGALS3* and clustered between the larger T_N and T_{EM} clusters and was deemed to represent T_{CM}.

The first three clusters accounted for more than 75% of all cells from both the BM and PB. However, differences in cluster distribution were evident: the dominant T_{EM} cluster as well as T_N and P_{RE}-EX clusters were enriched in the BM, whereas the T_{TE} cluster predominated the PB (Figure 1C). Single-cell gene set enrichment analysis (sc-GSEA) revealed enrichment towards the hallmark gene sets of hypoxia and tissue necrosis factor (TNF) α signaling via nuclear factor (NF)-$\kappa\beta$ in all but the T_N and T_{CM} clusters in the BM as compared to the PB (*Online Supplementary Figure S2B*), most evident in the dominant T_{EM} subset, but did not demonstrate overt inter-tissue differences with regards to other signaling or metabolic pathways (*Online Supplementary Table S5*).

An unsupervised, high-dimensional approach reveals inter-tissue differences highlighted by distinct Granzyme expression patterns

Inter-tissue differences were evident when stratifying clusters by the level of gene expression (Figure 2A; *Online Supplementary Table S6*), mainly restricted to genes that defined the T_{EM} and T_{TE} subsets (*Online Supplementary Figure S2C*), reflecting the compositional differences between these two tissue compartments. Although the T_N, T_{CM} and T_{TE} clusters demonstrated little to distinguish between BM and PB, BM-CD8+ T_{EM} demonstrated a greater level of both gene expression and proportion of cells expressing all genes that defined the cluster, except for *CD74* which was comparable

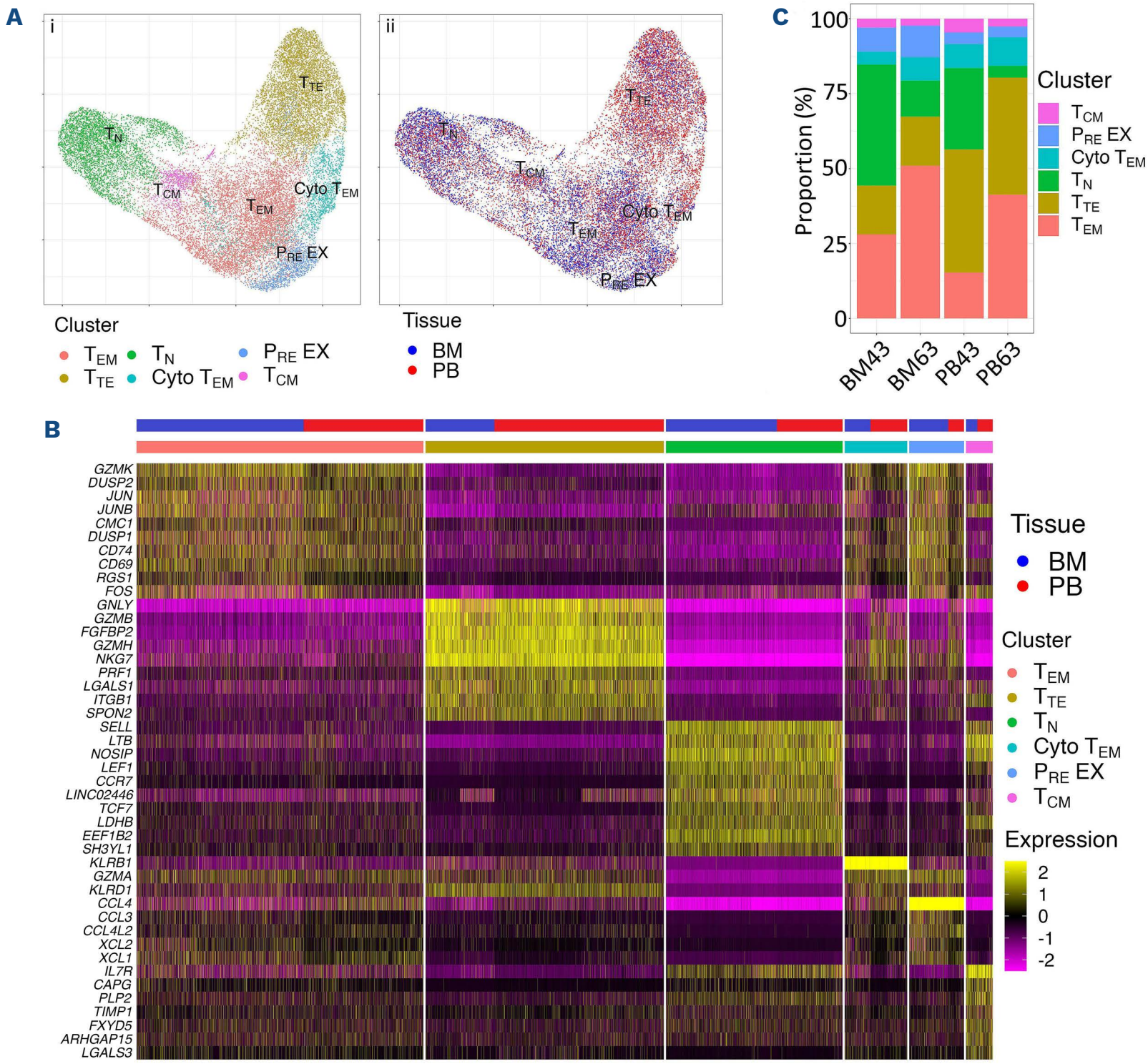

Figure 1. Distribution and quantification of CD8⁺ T-cell clusters found through unsupervised clustering. (A) Uniform Manifold Approximation and Projection (UMAP) of identified clusters. After stringent quality control (detailed in the *Online Supplementary Appendix*) revealed poor quality data for 2 bone marrow (BM) samples (excluded from further analysis), Seurat clustered CD8⁺ T cells from paired BM and peripheral blood (PB) of newly diagnosed multiple myeloma (NDMM) patients (N=2) into 6 clusters. Each dot represents a single cell colored according to (i) cluster or (ii) tissue compartment (BM = blue, PB = red). (B) Single-cell heat map illustrating transcriptional heterogeneity of CD8⁺ T cells. Each vertical line represents a single cell demonstrating the expression level, relative to the average expression level (upregulated = yellow, downregulated = purple) of the top 10 unique genes (y-axis) contributing to the transcriptional signature of each of the 6 identified clusters arranged by size of cluster (colored) and tissue (BM = blue, PB = red). (C) Bar plot quantifying cluster distribution. Quantification of the number of cells (y-axis) contributing to each identified cluster (color) from each of the contributing samples (x-axis). T_{EM}: effector memory T cells; T_{TE}: terminally differentiated CD8⁺ T cells; T_N: naive T cells; Cyto T_{EM}: cytotoxic effector memory T cells; P_{RE} EX: pre-exhausted T cells; T_{CM}: central memory T cells.

between the two tissues (Figure 2A; *Online Supplementary Figure S2C*). While the Cyto T_{EM} and P_{RE} EX clusters appear ontologically related, both showed marked differences between the BM and PB, with cells from BM co-expressing high levels of genes that defined the T_{EM} cluster and PB cells co-expressing genes that defined the T_{TE} cluster (Figure 2A; *Online Supplementary Figure S2C*). Quantification of the five human Granzymes revealed that while *GZMA*, *GZMH* and *GZMM* were similar between clusters within the BM and PB (*Online Supplementary Figure S2D*), *GZMK* was largely restricted to the BM and *GZMB* to the PB, with the exceptions of the PB T_{EM} and BM T_{TE} clusters respectively, which are non-dominant clusters in the PB and BM respectively (Figure 2B). Overlaying expression of several cluster-defining genes revealed a high level of co-expression of *CD69* and *GZMK*, largely restricted to the BM, while co-expression of

PRF1 demonstrated no overlap with *GZMK* but a high degree of overlap with *GZMB*, particularly in the PB (Figure 2C).

Flow cytometry reveals disease-associated differences

Flow cytometry was performed on paired BM and PB samples from NDMM patients and age-matched controls (N=12) to both determine if the same patterns observed in gene expression were reflected in protein expression and to query the effect of disease. CD69 protein expression was restricted to cells from the BM, with a small but not significant reduction in the proportion of CD8⁺ T cells expressing CD69 in NDMM patients relative to age-matched controls

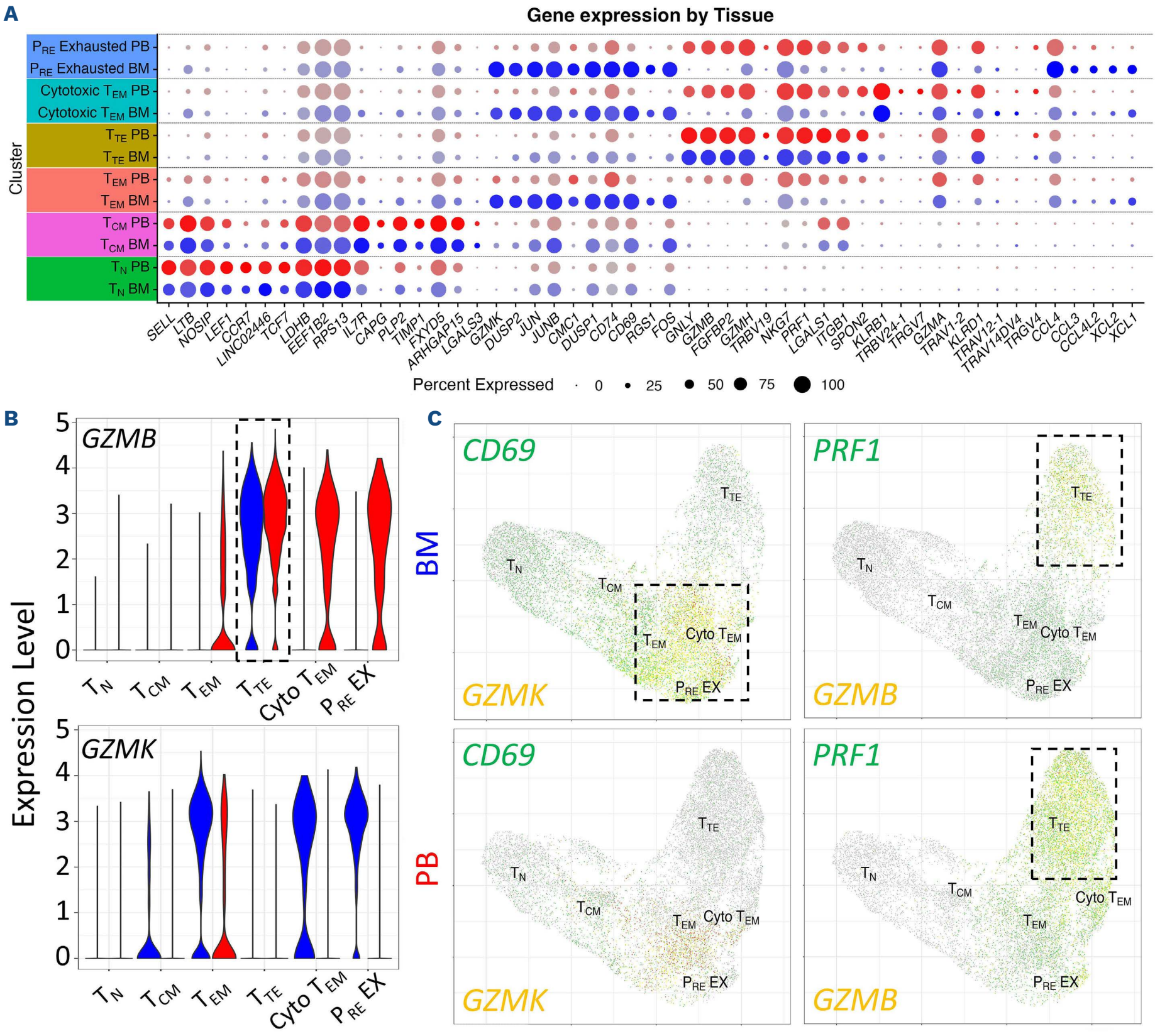

Figure 2. Unsupervised clustering reveals tissue restricted Granzyme expression patterns. (A) Dot plot illustrating the top 10 unique genes (x-axis) contributing to the identification of each of the 6 identified clusters (y-axis, colored, separated by tissue (bone marrow [BM] = blue, peripheral blood [PB] = red)). The size of each dot represents the percentage of cells within a cluster expressing a given gene and the intensity of the color represents the average expression level relative to the same cluster in the opposing tissue (solid = upregulated, transparent = downregulated). (B) Violin plots showing expression levels (y-axis) of *GZMB* (top) and *GZMK* (bottom) across the 6 identified clusters, separated by tissue (BM = blue, PB = red). The box highlights similar inter-tissue expression levels of *GZMB* in the T_{TE} cluster. (C) Uniform Manifold Approximation and Projection (UMAP) highlighting co-expression of Granzyme B and Granzyme K (orange) with CD69 and Perforin (green) in the BM (top) and PB (bottom). Boxes highlight clusters with high levels of co-expression (yellow). T_{EM}: effector memory T cells; T_{TE}: terminally differentiated CD8⁺ T cells; T_N: naive T cells; T_{CM}: central memory T cells.

(medians 41.4% and 53.8%; *P*=not significant [NS]) (Figure 3A; *Online Supplementary Figure S3A*). Canonical subset distribution across the two broad subsets within the BM demonstrated a reduction in T_N (medians 12.3% and 28.4%; *P*=NS), and a significant decrease in T_{CM} (medians 20.6% and 27.6%; *P*=0.0449), mirrored by a significant increase in T_{TE} (medians 30.4% and 10.6%; *P*=0.0023) in the CD8⁺CD69⁻ subset in NDMM patients relative to age-match controls, but no differences in the proportion of T_{EM} (Figure 3Bi). In contrast, the CD8⁺ T_{EM} subset accounted for the majority of

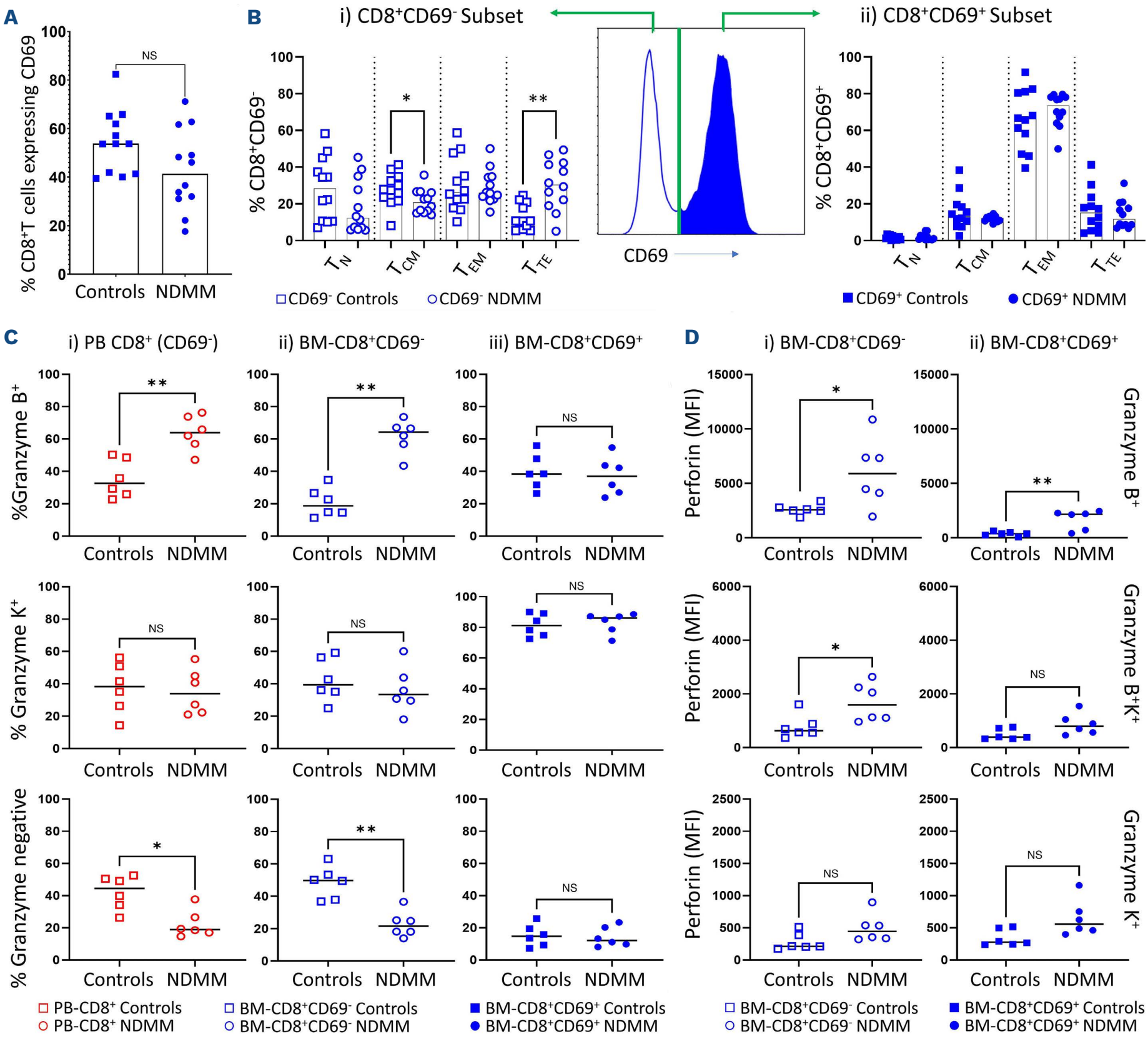

Figure 3. Tissue-restricted Granzyme expression patterns reveal disease-associated differences. (A) Quantification of the proportion of CD8⁺ T cells within the bone marrow (BM) co-expressing CD69 in age-matched controls (square; N=12) and newly diagnosed multiple myeloma (NDMM) patients (circles; N=12). (B) Quantification of canonical CD8⁺ T-cell subsets in the broad BM-CD8⁺CD69⁻ (i, open shapes) and BM-CD8⁺CD69⁺ (ii, solid shapes) subsets of age-matched controls (squares; N=12) and NDMM patients (circles; N=12). (C) Proportion of cells expressing Granzyme B (top), Granzyme K (middle) or Granzyme B⁻/K⁻ (bottom) in (i) PB-CD8⁺ (left; hollow red), (ii) BM-CD8⁺CD69⁻, (middle; hollow blue) and (iii) BM-CD8⁺CD69⁺, (right; solid blue) of age-matched controls (squares; N=6) and NDMM patients (circles; N=6). (D) Median fluorescence intensity (MFI) of Perforin expression across the Granzyme B⁺ (top) Granzyme B⁺/K⁺ (middle) or Granzyme K⁺ (bottom) subsets in (i) BM-CD8⁺CD69⁻ (left; hollow blue) and (ii) BM-CD8⁺CD69⁺ (right; solid blue) of age-matched controls (squares; N=6) and NDMM patients (circles; N=6). Significance levels: **P*<0.05, ***P*<0.01; Mann-Whitney U test. NS: not significant; T_{EM}: effector memory T cells; T_{TE}: terminally differentiated CD8⁺ T cells; T_N: naive T cells; T_{CM}: central memory T cells.

all CD8⁺CD69⁺ cells, however, no significant differences were observed between patient cohorts in any subset (Figure 3Bii). Contrasting the transcriptional assessment where cells expressed either *GZMB* or *GZMK*, flow cytometry revealed co-expression of both Granzyme B and Granzyme K in both NDMM patients and age-matched controls (*Online Supplementary Figure S3A*). NDMM patients demonstrated a significant increase in the proportion of both BM-CD8⁺CD69⁻ (median 64.3 *vs.* 18.7%; *P*=0.022) and PB-CD8⁺ T cells (median 64.0 *vs.* 32.5%; *P*=0.0087) expressing Granzyme B compared to age-matched controls, paralleled by significantly fewer Granzyme-negative cells in these two subsets (median 21.5 *vs.* 49.8%; *P*=0.022) (median 19.0 *vs.* 44.5%; *P*=0.0152) (Figure 3Ci, ii). Further, Granzyme B expression patterns in the BM-CD8⁺CD69⁻ subset of NDMM patients mimicked expression patterns observed in the PB closer than age-matched controls (average ratio of BM-CD8⁺CD69⁻: PB-CD8⁺: 1.01 *vs.* 0.36 NDMM patients *vs.* age-matched controls; *P*=0.026) (*Online Supplementary Figure S3B*). In contrast, while Granzyme K was largely restricted to the BM-CD69⁺ subset (though not exclusive), the expression did not differ between health and disease (Figure 3Ciii). Overall, while marked differences in Granzyme expression patterns were observable between patient cohorts in both the PB-CD8⁺ (*Online Supplementary Figure S3Ci*) and BM-CD8⁺CD69⁻ subsets (*Online Supplementary Figure S3Cii*), the BM-CD8⁺CD69⁺ subset appeared almost identical (*Online Supplementary Figure S3C iii*). Compositional alterations of the BM-CD8⁺CD69⁻ subset in MM were further reinforced by analysis of canonical subset distribution, where a significant difference (*P*=0.0312) in the distribution of T_{TE} was observable between the two BM subsets in NDMM, but not in age-matched controls (*Online Supplementary Figure S3D*).

In keeping with compositional similarities of Granzyme expression, perforin expression in the BM-CD8⁺CD69⁻ subset appeared to mimic that observed in the PB in NDMM patients, but not age-matched controls (Figure 3D; *Online Supplementary Figure S4A*). While perforin expression was higher in all Granzyme subsets in the PB-CD8⁺ subset of NDMM patients (*Online Supplementary Figure S4B*), it was significantly higher in Granzyme B-expressing cells in the BM-CD8⁺CD69⁻ subset (Figure 3Di); applying to both Granzyme B single positive (average median fluorescence intensity [ave. MFI] 5,907 *vs.* 2,567; *P*=0.0411) and Granzyme B⁺/K⁺ (ave. MFI 1,590 *vs.* 699; *P*=0.0158) cells. Although BM-CD8⁺CD69⁺GZB⁺T cells consisted of only a minority of cells in both cohorts, NDMM patients again demonstrated a marked increase in perforin expression compared to age-matched controls (ave. MFI 377 *vs.* 2,175; *P*=0.0087) (Figure 3Dii).

Mass cytometry demonstrates CD8⁺CD69⁺ effector memory T cells are phenotypically restrained relative to their CD69⁻ counterparts

In order to obtain a more comprehensive phenotype, and further interrogate the effect of the microenvironment on the BM-dominant T_{EM} subset, we performed FlowSOM analysis[14] of paired BM and PB samples from MGUS and NDMM patients. This revealed four metaclusters enriched in the BM

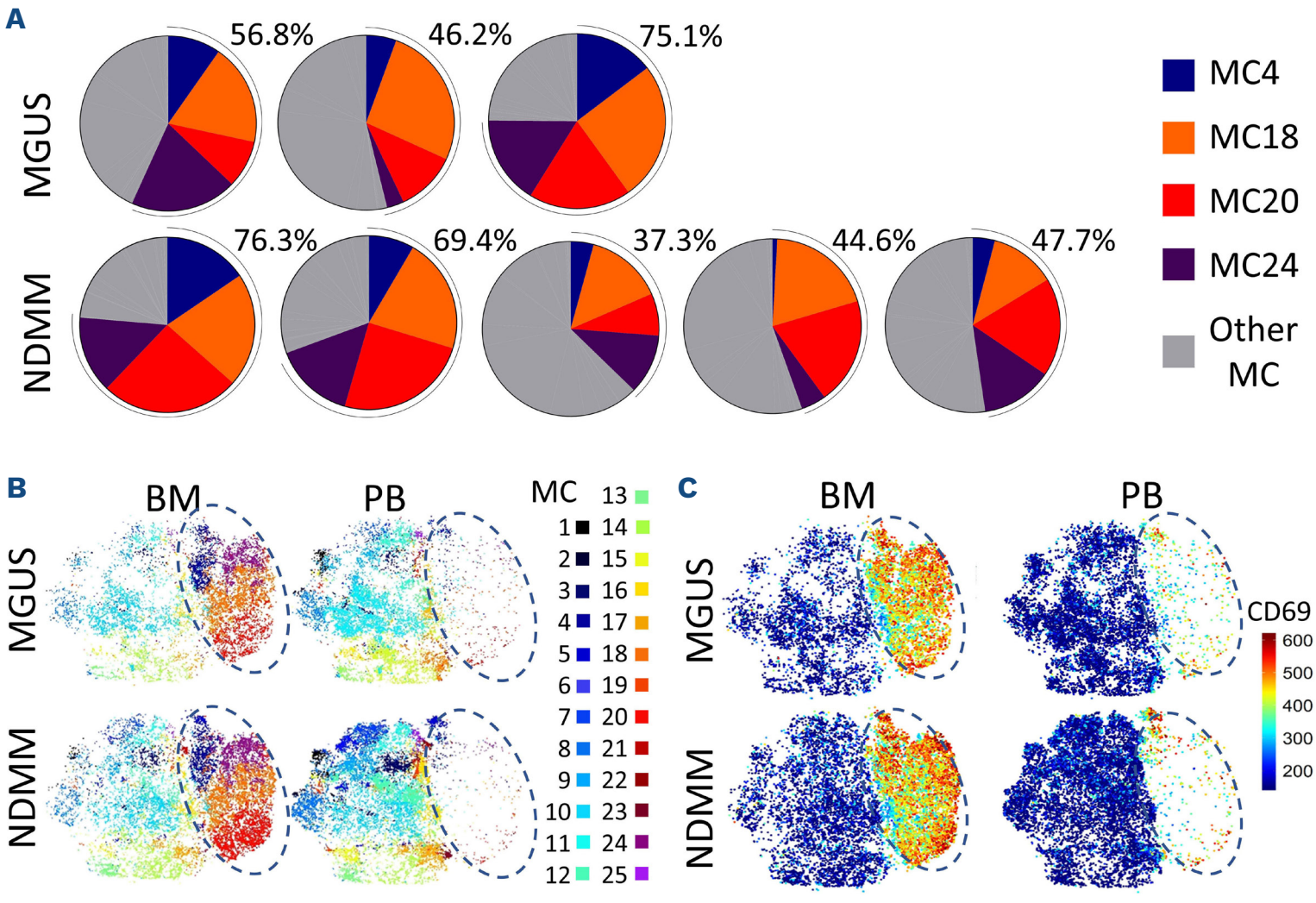

Continued on following page

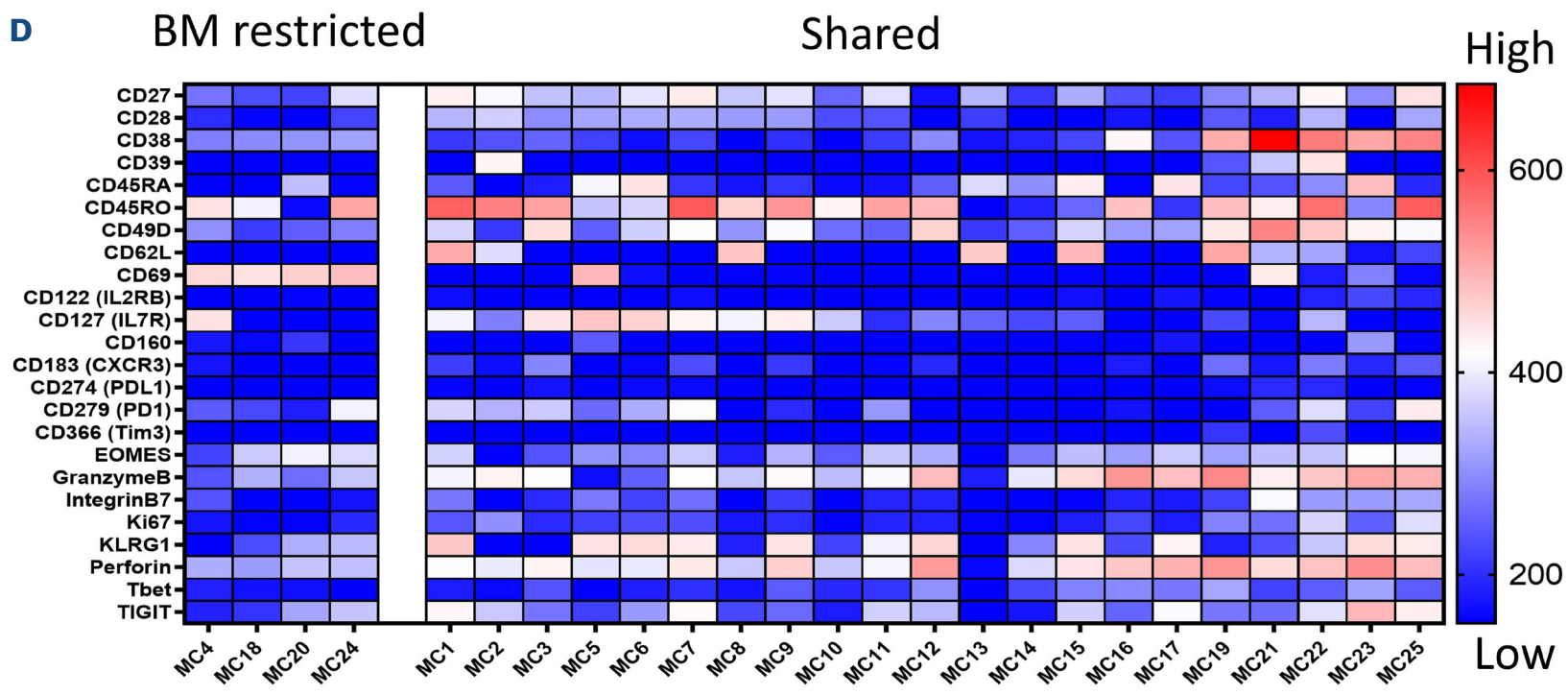

Figure 4. Bone marrow-restricted CD8⁺CD69⁺ effector memory T cells are phenotypically restrained compared to cells shared between bone marrow and peripheral blood. (A) Pie charts showing the contribution of the 4 metacluster (MC) (MC4: blue, MC18: orange, MC20: red and MC24: purple) overrepresented in the bone marrow (BM) of monoclonal gammopathy of undetermined significance (MGUS) (top) and newly diagnosed multiple myeloma (NDMM) (bottom) patients (remaining MC: grey). (B) t-distributed stochastic neighbour embedding (tSNE) visualization of identified MC within the BM (left) and peripheral blood (PB) (right) in MGUS (top) and NDMM (bottom) patients. The right half of each plot is occupied entirely by 4 MC (highlighted by the dark blue dashed ovals). Each dot represents an individual cell, colored by the assigned MC. (C) tSNE visualization of CD69 expression showing restriction to the same region that encompasses the 4 BM-restricted MC, colored by the level of expression from low (blue) to high (red). (D) Heat map showing the phenotype of the 25 MC. MC4, MC18, MC20, and MC24 contain CD69⁺ effector memory T cells (T_{EM}) (left) are BM-restricted, with the remaining 21 MC shared between BM and PB. The color represents the median intensity of the signal from low (blue) to high (red) for an individual marker (row) in an individual MC (column).

of both MGUS and NDMM (Figure 4A). Visualization of cluster distribution on t-distributed stochastic neighbor embedding (tSNE) (Figure 4B) revealed these four metaclusters as cells expressing high levels of CD69 (Figure 4C), confirming tissue-restricted expression of this protein. Despite accounting for approximately half of all cells in both cohorts, FlowSOM determined these cells sufficiently homogeneous as to cluster them into only four metaclusters, suggesting the bulk of phenotypic heterogeneity exists across the 21 metaclusters shared between BM and PB (Figure 4D).

Flow cytometry demonstrates enhanced levels of CD38 and CD69 differentiate health and disease within the bone marrow-CD8⁺CD69⁺ population

Focusing on differences within the BM, FlowSOM analysis of high dimensional flow cytometry data of the BM-CD8⁺ T_{EM} subset revealed differences between MM and age-matched controls were largely restricted to levels of expression of markers associated with TCR-activation, CD38 and CD69, but not CD25 (Figure 5A). However, differences were not restricted to the dominant CD8⁺ T_{EM} subset, with manual analysis revealing significantly higher levels of CD69 expression evident in MM compared to age-matched controls evident across all antigen-experienced cells (Figure 5B). CD38 was similarly expressed at significantly higher levels in all canonical subsets in both the BM-CD8⁺CD69⁻ and BM-CD8⁺CD69⁺ T cells in MM (Figure 5C). Analysis of inhibitory markers PD-1 and TIGIT revealed disease-associated differences evident only within the CD69⁻ subset; BM-CD8⁺CD69⁻ T_{TE} demonstrated significantly fewer cells expressing PD-1 in MM compared to age-matched controls (Figure 5D). Similarly, significantly fewer BM-CD8⁺CD69⁻ T_{EM} and T_{TE} expressed TIGIT in MM compared to age-matched controls (Figure 5E).

Broad dissimilarities between BM-CD8⁺CD69⁻ and BM-CD8⁺CD69⁺ T_{EM} subsets were evident in expression patterns of the interleukin-7 receptor α (IL-7R/CD127) and killer cell lectin-like receptor G1 (KLRG1), markers associated with effector/memory distinction,[15] with a marked reduction in cells expressing CD127 in the BM-CD8⁺CD69⁺ subset (*Online Supplementary Figure S4C*). However, there were no significant differences between cohorts (*Online Supplementary Figure S4D*). Finally, assessment of TCF-1 expression, a transcription factor crucial in the maintenance of "stemness" in the TME[16] across canonical subsets within the BM demonstrated no disease-associated differences (*Online Supplementary Figure S4E*).

Bone marrow-CD8⁺ T cells from newly diagnosed multiple myeloma patients share compositional similarity to T-cell receptor-activated age-matched controls

Generation of reference atlases from the BM of two (*Online Supplementary Figure S5A*) and PB of four (*Online Supplementary Figure S5B*) NDMM patients, using the R package

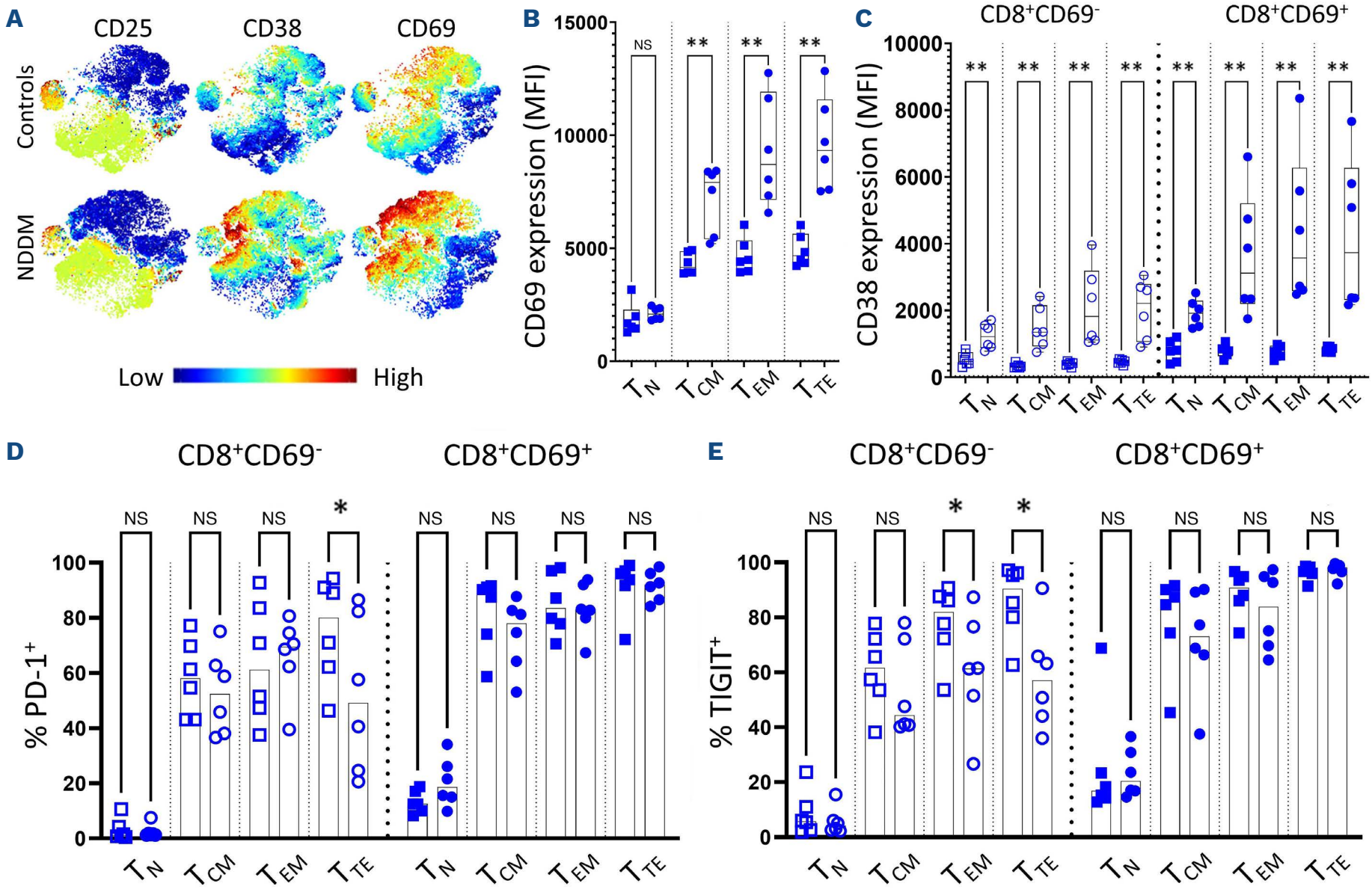

Figure 5. Bone marrow-CD8⁺CD69⁺ T cells demonstrate an activated phenotype in multiple myeloma. (A) t-distributed stochastic neighbour embedding (tSNE) plots of FlowSOM clustered bone marrow CD8⁺ effector memory T cells (BM-CD8⁺ T_{EM}) showing expression of CD25 (left), CD38 (middle) and CD69 (right) in the BM of age-matched controls (top) and newly diagnosed multiple myeloma (NDMM) patients (bottom). Each dot represents a single cell, the scale shows the level of expression of each marker from low (blue) to high (red). (B) Median fluorescence intensity (MFI) of CD69 expression on the 4 canonical CD8⁺ T-cell subsets of the CD8⁺CD69⁺ subset between age-matched controls (squares) and NDMM patients (circles). (C) MFI of CD38 expression on the 4 canonical CD8⁺ T-cell subsets within the broad BM-CD8⁺CD69⁻ (left, open shapes) and BM-CD8⁺CD69⁺ (right, solid shapes) subsets between age-matched controls (squares) and NDMM patients (circles). (D, E) Bars (median with scatter) showing proportions of T_N, T_{CM}, T_{EM} and T_{TE} in the broad BM-CD8⁺CD69⁻ (left, open shapes) and BM-CD8⁺CD69⁺ (right, solid shapes) subsets expressing (D) PD-1 and (E) TIGIT in age-matched controls (squares) and NDMM patients (circles). Significance levels: *P<0.05, **P<0.01; Mann-Whitney U test. MC: metacluster; T_{TE}: terminally differentiated CD8⁺ T cells; T_N: naive T cells; Cyto T_{EM}: cytotoxic effector memory T cells; P_{RE} EX: pre-exhausted T cells; T_{CM}: central memory T cells; NS: not significant.

"ProjecTILs", permitted unbiased comparisons with age-matched control data.[13] Atlases comprised of 6,275 cells from each input sample and captured a total of 16,316 and 16,840 genes respectively. Both atlases formed six clusters comprising transcriptionally similar T_{EM}, T_{TE} and T_N clusters observable in the integrated analysis as well as a more evident *IL7R*⁺ memory cluster (designated IL7R⁺ T_M) and a smaller cluster of activated cells defined by high levels of the *HLA-DR* family of genes.[17] Unique to each atlas was one small cluster; a Cyto-T_{EM} like cluster in the BM, with high levels of *KLRD1*, *KLRC3* and *KIR3DL2* and a IFN-stimulated cluster in the PB.

Comparing generated atlases against resting and TCR-activated CD8⁺ T cells from the BM and PB of age-matched controls[18] revealed resting BM cells predominantly clustering into the dominant T_{EM} cluster, then equally into the IL7R⁺ T_M and T_{TE} clusters, whereas resting cells from PB skewed toward the dominant T_{TE} cluster. TCR activation induced marked compositional changes evident only in the BM (Figure 6A), such that clustering was near exclusive to the dominant T_{EM} cluster, whilst few compositional differences were observed in the PB (*Online Supplementary Figure S6A*).

Sc-GSEA revealed that the previous BM enrichment towards hypoxia and TNFα signaling via NF-κβ were attributable to micro-environmental differences between health and disease, rather than differences between the two tissue compartments alone: while TCR activation of BM-CD8⁺ T cells induced slight enrichment towards these two gene sets, both were markedly higher in myeloma (*Online Supplementary Figure S7A*; *Online Supplementary Table S7*). In

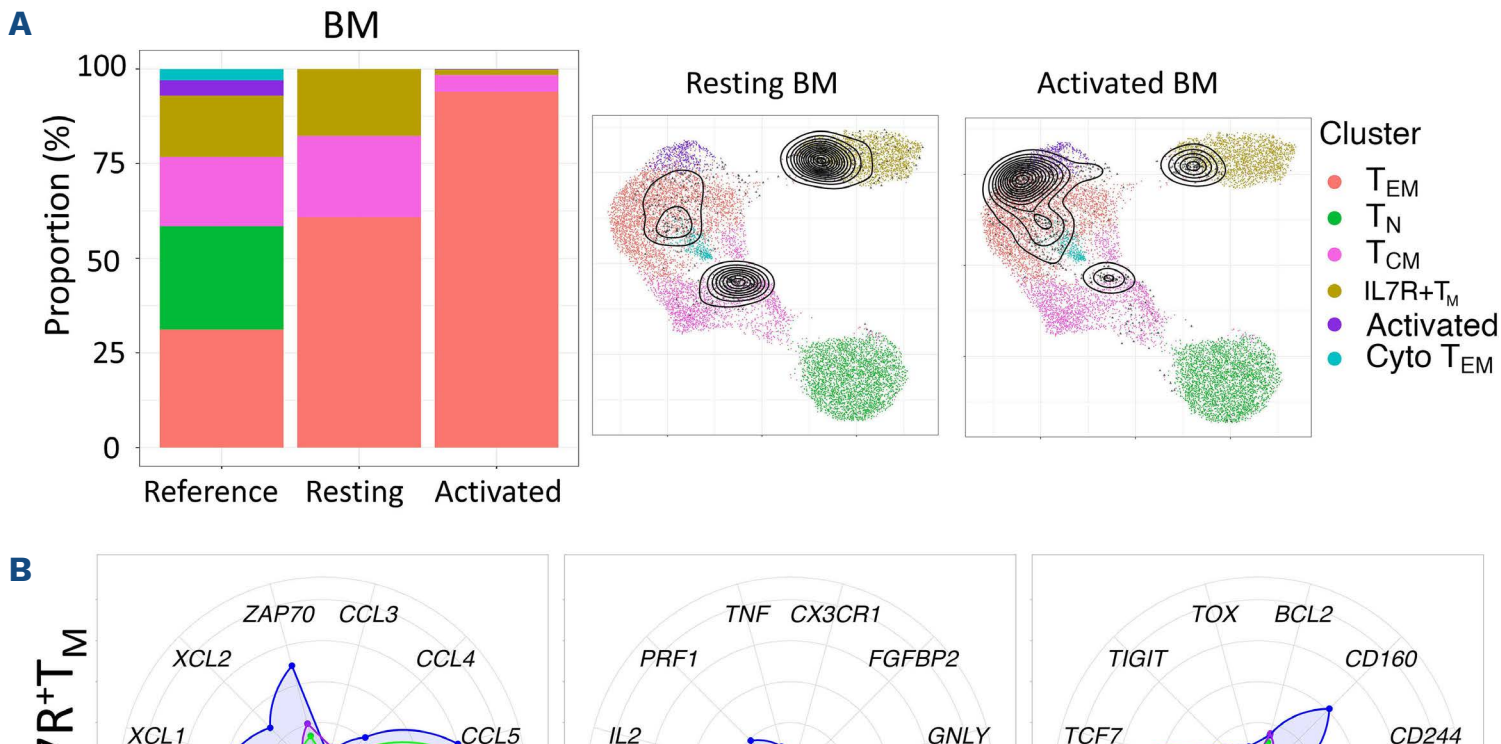

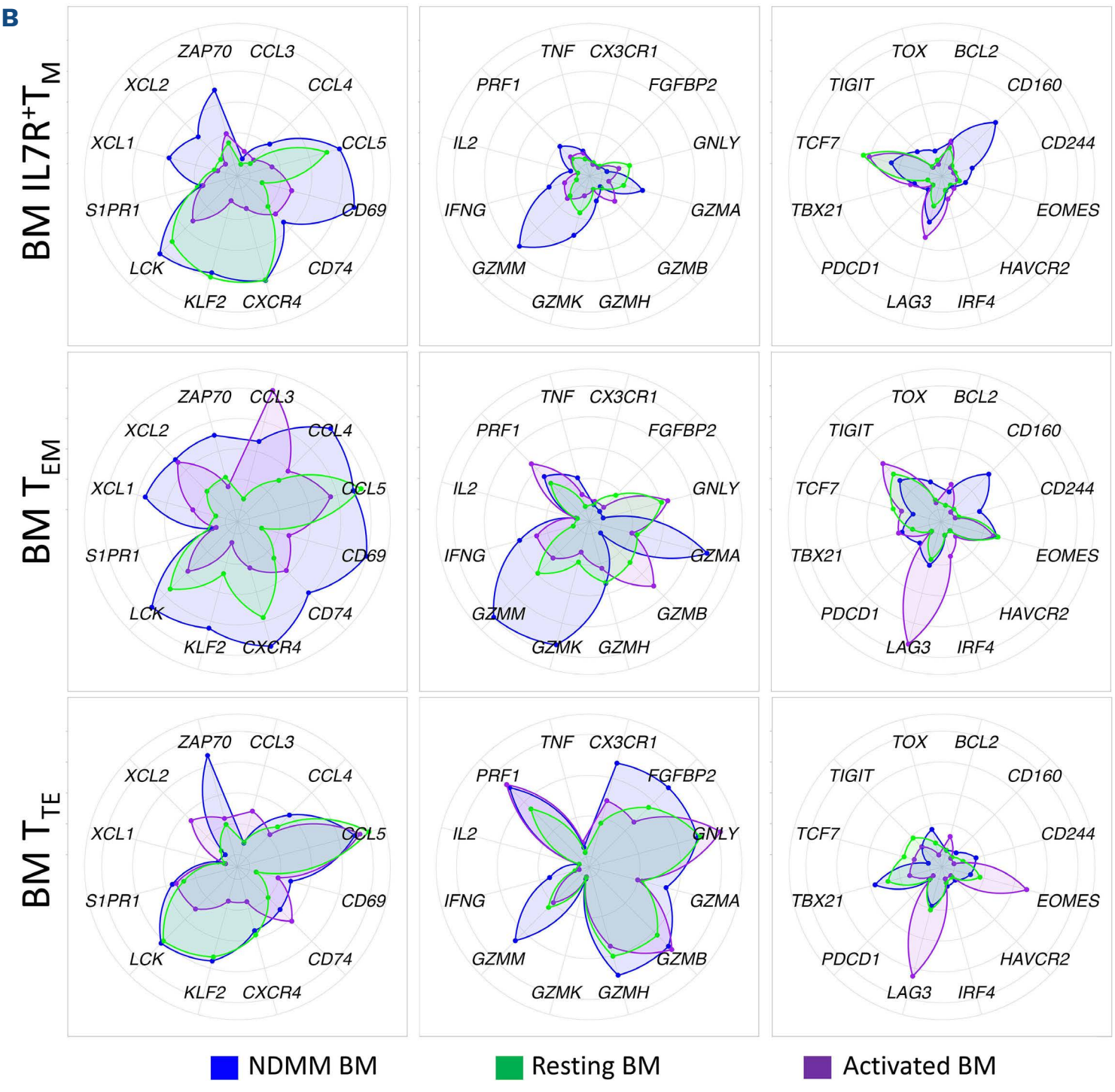

Figure 6. Bone marrow-CD8⁺ T cells in multiple myeloma transcriptionally resemble T-cell receptor-activated cells from healthy donors. (A) ProjecTILs clustered CD8⁺ T cells from the bone marrow (BM) of newly diagnosed multiple myeloma (NDMM) patients (N=2) into 6 clusters. Each dot represents a single cell colored according to cluster. Contour plots represent distribution of CD8⁺ T cells from age-matched control data in resting (left) or T-cell receptor (TCR)-activated states (right). The stacked bar graph illustrates cluster distribution of the reference atlas or controls data in resting (left) or TCR-activated states (right). (B) Radar plots demonstrating expression levels of key genes related to TCR-activation and chemotaxis (left), effector function (middle) and T-cell exhaustion/transcriptional regulators (right) of CD8⁺ T cells from age-matched controls in TCR-activated (purple) or resting state (green) relative to the NDMM BM reference (blue) across the IL7R⁺ T_M (top), T_{EM} (middle) and T_{TE} clusters (bottom). T_{EM}: effector memory T cells; T_{TE}: terminally differentiated $CD8_+$ T cells; T_N: naive T cells; Cyto T_{EM}: cytotoxic effector memory T cells; IL7R+ T memory cells.

contrast, while TCR activation did not result in enrichment towards hypoxia in the PB, it induced enrichment in TNFα signaling via NF-κβ above the myeloma reference (*Online Supplementary Figure S7B*; *Online Supplementary Table S7*). Differential expression testing of the dominant T_{EM} cluster comparing resting and TCR-activated age-matched cells from the BM to the MM reference indicated TCR activation induced marked changes, including upregulation of many expected genes such as *CD69*, *CD74*, *GZMB*, *IL2RA* and *IL2RG*, relative to the MM reference (*Online Supplementary Table S8A*). Comparisons of age-matched cells from the PB to the dominant MM PB T_{TE} showed TCR activation-induced upregulation of several chemokine ligands (*CCL3*, *CCL4*, *XCL1* and *XCL2*) and, contrasting cells from the BM, upregulation of several AP-1 associated genes (e.g., *JUNB*, *DUSP2*) (*Online Supplementary Table S8B*).

Finally, relative expression of key genes across the IL7R+ T_M, T_{EM} and T_{TE} clusters of the BM (Figure 6B) and PB (*Online Supplementary Figure S6B*) demonstrated that although TCR activation induced upregulation of several genes associated with T-cell activation relative to resting cells, only *CCL3* was consistently expressed at a higher level than the MM reference. Expression of all Granzymes, except for *GZMB*, was higher in the MM reference than in either TCR-activated or resting cells from age-matched controls, while *PRF1* expression in TCR-activated cells demonstrated similar expression patterns to the MM reference. NDMM BM T_{EM} demonstrated markedly higher levels of many inflammatory-associated chemokine genes including *XCL1*, *XCL2*, *CCL4* and *CXCR4* than either resting or TCR-activated age-matched samples and, suggestive of highly differentiated cells, NDMM T_{TE} in both the BM and PB demonstrated higher levels of *CX3CR1* relative to age-matched controls. Low levels of inhibitory markers were evident across all subsets, however, TCR activation induced expression of *LAG3* and *HAVCR2* and *IRF4* in all but the BM T_{TE} subset, which demonstrated a marked increase in *EOMES*. In keeping with flow assessment of TCF-1, no notable differences were evident in the expression of *TCF7* in the BM.

Discussion

The tumor microenvironment has a demonstrable impact on the function and clonal composition of CD8+ T cells in both solid cancers[19] and several hematological malignancies,[20,21] but remains under investigation in MM. Previous reports have suggested that T cells exhibit signs of exhaustion[22] and senescence in the TME[23] but few have focused in depth on differences between clonal T cells across the BM and PB. In this study, we utilized several single-cell technologies to probe tumor-induced differences in CD8+ T cells in NDMM patients. Using an unsupervised approach, we found several clusters aligned with canonical T-cell maturation shared between the BM and PB, with no tissue or patient-restricted clusters evident. Inter-tissue differences were evident in the differential expression of Granzyme B and Granzyme K, which were strongly associated with two distinct subsets of CD8+ T cells delineated by the expression of CD69, accounting for roughly 50% of all T cells in the BM of both health and disease. While the CD69- subset in NDMM patients demonstrated a marked skewing towards more differentiated cells compared to age-matched controls, the CD69-positive subset was comprised primarily of T_{EM} with a similar expression between NDMM and controls. Given the restriction to the BM and the established role of CD69 as a marker of tissue residency,[24] it is reasonable to assume that the CD69+ population is resident within the BM, whereas the CD69- subset represents an infiltrating, or circulating population. Thus, alterations in both canonical subset distribution and Granzyme B and Granzyme K expression patterns observed in MM may represent either an influx of more differentiated cells responding to an altered chemokine gradient within the inflamed marrow, an expedited differentiation of cells into a more potent effector-like cell or both.

Expression of Granzyme B and Granzyme K in the BM-CD8+CD69- T-cell subset of NDMM patients demonstrated increased representation of highly differentiated effector cells and evident compositional parallels to PB CD8+ T cells, contrasting a marked reduction of effector cells in age-matched controls. This may indicate greater infiltration of the BM microenvironment by Granzyme B-positive CD8+CD69- T cells in NDMM than age-matched controls. Phase I clinical trial results of Teclistamab[25] and Talquetamab[26] suggest the pool of highly potent effector cells with low levels of co-inhibitory molecules evident in the MM TME are therapeutically exploitable, irrespective of innate TCR specificity. In our study, *GZMK* expression was strongly associated with *CD69* expression in the BM. Further, we observed upregulation of several chemokine ligands, suggesting a role for these cells as not only potential inflammatory mediators but as chemoattractant cells. While Granzyme B has an established role in cytotoxicity,[27] far less is known about the role of Granzyme K,[28] and less still about its role in MM. Increased frequencies of Granzyme K+CD8+ T cells have been detected in inflamed tissue, and their presence correlates with increased plasma levels of IL-6, IL-8 and TNFα.[29] Granzyme K+CD8+ T cells were recently identified as hallmarks of "inflammaging",[29] and have been demonstrated to induce both IL-6 and IL-8 expression in stromal cells,[30] potentially contributing to the pathophysiology of myeloma as inflammatory mediators are well-established drivers of disease.[31] The classification of these cells is a current point of contention in MM: De Jong *et al*, postulated that a Granzyme K+CD8+ T-cell subset was partially responsible for increased levels of inflammation in the MM TME,[32] whereas *GZMK*+ cells have been referred to as 'protective memory' by Zavidij *et al.*[33] In keeping with recent findings by Bailur *et al.*,[34] we did not observe differences between health and disease in the expression of either *TCF7* or the protein it

encodes. The lack of observable differences between health and disease in both proportions of Granzyme K⁺CD8⁺ T cells, TCF-1 expression (as well as other relevant genes e.g., *BCL2* and *TOX*) and lack of difference in the enrichment of the Wnt-β-catenin signaling pathway, as analyzed by sc-GSEA (*Online Supplementary Table S7*), suggests CD8⁺ T-cell memory maintenance in MM may not be impeded to a significant level. Rather, the perceived reduction of 'protective memory' may be attributable to proportional skewing towards a more differentiated phenotype within the TME, rather than a reduction in absolute numbers as more 'space' within the BM is repurposed for malignant PC growth.

The BM-dominant CD8⁺CD69⁺ T_{EM} subset was phenotypically similar in age-matched controls and NDMM, except for increased expression levels of CD69 and CD38 in NDMM, observable across all antigen-experienced T cells. While upregulated CD38 may render these cells susceptible to the on-target, off-tumor action of Daratumumab,[35] upregulated CD69 on BM CD8⁺ T cells in NDMM is intriguing. CD69 is a multifunctional protein with at least four known ligands.[36] Of these, galectin-1 (gal-1) is highly relevant to MM given its established role in T-cell responses and over-representation in the NDMM extracellular matrix.[37] Over-representation of gal-1 in MM may be due to overexpression by both malignant PC, with expression upregulated in response to hypoxia,[38] but also degranulation by cytotoxic T cells.[39] Upregulated CD69 may also imply a greater likelihood of cells remaining within the marrow as CD69 functions to inhibit cell egress to the periphery.[24,36] Although recent data suggests accumulation of CD8⁺CD69⁺ T cells within the MM TME is associated with an increase in progression-free survival,[40] reduced *GZMB* is associated with rapid disease progression.[22] *CD69* is a direct hypoxia-inducible factor 1-α (HIF-1 α) target gene.[41] This may suggest that the CD69 expression observable in the BM may be associated with cellular stress, chiefly hypoxia-related, either in addition to or, rather than, T-cell activation. While hypoxia can to negatively impact CD8⁺ T-cell function, it can, conversely, enhance effector CD8⁺ T-cell response to persistent antigens.[42] In this respect, hypoxia enhances T_{EM} proliferation through a positive feedback loop involving HIF-1α and glycolysis.[43] GSEA revealed differences in enrichment towards the hallmark gene set of glycolysis between health and disease in the T_{EM} subset of the BM (*Online Supplementary Table S7*), however the low levels of Ki67 (evident by mass cytometry) suggest these cells are quiescent. Preliminary functional work has demonstrated robust cytokine production and capacity to degranulate in both CD69⁺/⁻ subsets in both NDMM patients and age-matched controls upon magnetic bead stimulation (*data not shown*) reinforcing our previous findings,[12] however further clarification of the role of CD8⁺CD69⁺ T cells as a resident memory pool within the MM TME is required. Finally, clonally restricted cells have been observed in both CD8⁺CD69⁺ and CD8⁺CD69⁻ T-cell subsets, and their cognate antigens are under investigation.

Disclosures

No conflicts of interest to disclose

Contributions

JF and CEB designed and performed the research, analyzed the data, wrote the human ethics and wrote the paper. EA and SY performed the research and analyzed the data. SG assisted with the bioinformatics and analyzed the data. NN and LMS assisted in research design and data analyis. CEB, EA, TK, and PJH assisted in research design, reviewed patients, and assisted with the collection of patient samples and clinical information. RB reviewed patients undergoing hip arthroplasty and designed research. DJ and PJH were involved in research design, analysis of data and writing the paper.

Acknowledgments

The authors thank Dr Alberto Catalano for excellent research management support, RPAH Hematology Clinicians for collection of patient samples and informed consent, and patients and their families for donating samples for research. They would also like to thank Prof Joseph Powell and Dr Walter Muscovic from the Garvan-Weizmann Center for Cellular Genomics as well as Dr Slavica Vuckovic for their contributions in the earlier stages of this project.

Funding

This work is funded by a Brian D. Novis research grant from the International Myeloma Foundation (to CEB) and Sydney Blood Cancer Research.

Data-sharing statement

Data may be made available by contacting the corresponding author.

References

1. Rajkumar SV. Multiple myeloma: 2020 update on diagnosis, risk-stratification and management. Am J Hematol. 2020;95(5):548-567.
2. Wang H, Leng Y, Gong Y. Bone marrow fat and hematopoiesis. Front Endocrinol (Lausanne). 2018;9:694.
3. Di Rosa F, Gebhardt T. Bone marrow T cells and the integrated functions of recirculating and tissue-resident memory T cells. Front Immunol. 2016;7:51.
4. Lightman SM, Utley A, Lee KP. Survival of long-lived plasma cells (LLPC): piecing together the puzzle. Front Immunol. 2019;10:965.
5. Bruns I, Cadeddu RP, Brueckmann I, et al. Multiple myeloma-related deregulation of bone marrow-derived CD34(+) hematopoietic stem and progenitor cells. Blood. 2012;120(13):2620-2630.
6. Gooding S, Olechnowicz SWZ, Morris EV, et al. Transcriptomic profiling of the myeloma bone-lining niche reveals BMP signalling

inhibition to improve bone disease. Nat Commun. 2019;10(1):4533.
7. Vuckovic S, Minnie SA, Smith D, et al. Bone marrow transplantation generates T cell-dependent control of myeloma in mice. J Clin Invest. 2019;129(1):106-121.
8. Bryant C, Suen H, Brown R, et al. Long-term survival in multiple myeloma is associated with a distinct immunological profile, which includes proliferative cytotoxic T-cell clones and a favourable Treg/Th17 balance. Blood Cancer J. 2013;3(9):e148.
9. Suen H, Brown R, Yang S, et al. Multiple myeloma causes clonal T-cell immunosenescence: identification of potential novel targets for promoting tumour immunity and implications for checkpoint blockade. Leukemia. 2016;30(8):1716-1724.
10. Suen H, Brown R, Yang S, Ho PJ, Gibson J, Joshua D. The failure of immune checkpoint blockade in multiple myeloma with PD-1 inhibitors in a phase 1 study. Leukemia. 2015;29(7):1621-1622.
11. Shah N, Chari A, Scott E, Mezzi K, Usmani SZ. B-cell maturation antigen (BCMA) in multiple myeloma: rationale for targeting and current therapeutic approaches. Leukemia. 2020;34(4):985-1005.
12. Vuckovic S, Bryant CE, Lau KHA, et al. Inverse relationship between oligoclonal expanded CD69- TTE and CD69+ TTE cells in bone marrow of multiple myeloma patients. Blood Adv. 2020;4(19):4593-4604.
13. Andreatta M, Corria-Osorio J, Müller S, Cubas R, Coukos G, Carmona SJ. Interpretation of T cell states from single-cell transcriptomics data using reference atlases. Nat Commun. 2021;12(1):2965.
14. Van Gassen S, Callebaut B, Van Helden MJ, et al. FlowSOM: using self-organizing maps for visualization and interpretation of cytometry data. Cytometry A. 2015;87(7):636-645.
15. Remmerswaal EBM, Hombrink P, Nota B, et al. Expression of IL-7Rα and KLRG1 defines functionally distinct CD8(+) T-cell populations in humans. Eur J Immunol. 2019;49(5):694-708.
16. Wen S, Lu H, Wang D, Guo J, Dai W, Wang Z. TCF-1 maintains CD8(+) T cell stemness in tumor microenvironment. J Leukoc Biol. 2021;110(3):585-590.
17. Saraiva DP, Azeredo-Lopes S, Antunes A, et al. Expression of HLA-DR in cytotoxic T lymphocytes: a validated predictive biomarker and a potential therapeutic strategy in breast cancer. Cancers. 2021;13(15):3841.
18. Szabo PA, Levitin HM, Miron M, et al. Single-cell transcriptomics of human T cells reveals tissue and activation signatures in health and disease. Nat Commun. 2019;10(1):4706.
19. Goulart MR, Stasinos K, Fincham REA, Delvecchio FR, Kocher HM. T cells in pancreatic cancer stroma. World J Gastroenterol. 2021;27(46):7956-7968.
20. Abbas HA, Hao D, Tomczak K, et al. Single cell T cell landscape and T cell receptor repertoire profiling of AML in context of PD-1 blockade therapy. Nat Commun. 2021;12(1):6071.
21. Nath K, Law SC, Sabdia MB, et al. Intra-tumoral CD8+ T-cells in follicular lymphoma contain large clonal expansions that are amenable to dual-checkpoint blockade. Blood. 2019;134(Suppl 1):2793.
22. Pilcher W, Thomas BE, Bhasin SS, et al. Characterization of T-cell exhaustion in rapid progressing multiple myeloma using cross center Scrna-Seq study. Blood. 2021;138(Suppl 1):401.
23. Zelle-Rieser C, Thangavadivel S, Biedermann R, et al. T cells in multiple myeloma display features of exhaustion and senescence at the tumor site. J Hematol Oncol. 2016;9(1):116.
24. Kumar BV, Ma W, Miron M, et al. Human tissue-resident memory T cells are defined by core transcriptional and functional signatures in lymphoid and mucosal sites. Cell Rep. 2017;20(12):2921-2934.
25. Moreau P, Garfall AL, van de Donk N, et al. Teclistamab in relapsed or refractory multiple myeloma. N Engl J Med. 2022;387(6):495-505.
26. Chari A, Minnema MC, Berdeja JG, et al. Talquetamab, a T-cell-redirecting GPRC5D bispecific antibody for multiple myeloma. N Engl J Med. 2022;387(24):2232-2244.
27. Voskoboinik I, Whisstock JC, Trapani JA. Perforin and granzymes: function, dysfunction and human pathology. Nat Rev Immunol. 2015;15(6):388-400.
28. Harari A, Bellutti Enders F, Cellerai C, Bart PA, Pantaleo G. Distinct profiles of cytotoxic granules in memory CD8 T cells correlate with function, differentiation stage, and antigen exposure. J Virol. 2009;83(7):2862-2871.
29. Mogilenko DA, Shpynov O, Andhey PS, et al. Comprehensive profiling of an aging immune system reveals clonal GZMK(+) CD8(+) T cells as conserved hallmark of inflammaging. Immunity. 2021;54(1):99-115.
30. Cooper DM, Pechkovsky DV, Hackett TL, Knight DA, Granville DJ. Granzyme K activates protease-activated receptor-1. PLoS One. 2011;6(6):e21484.
31. Musolino C, Allegra A, Innao V, Allegra AG, Pioggia G, Gangemi S. Inflammatory and anti-inflammatory equilibrium, proliferative and antiproliferative balance: the role of cytokines in multiple myeloma. Mediators Inflamm. 2017;2017:1852517.
32. de Jong MME, Kellermayer Z, Papazian N, et al. The multiple myeloma microenvironment is defined by an inflammatory stromal cell landscape. Nat Immunol. 2021;22(6):769-780.
33. Zavidij O, Haradhvala NJ, Mouhieddine TH, et al. Single-cell RNA sequencing reveals compromised immune microenvironment in precursor stages of multiple myeloma. Nat Cancer. 2020;1(5):493-506.
34. Bailur JK, McCachren SS, Doxie DB, et al. Early alterations in stem-like/resident T cells, innate and myeloid cells in the bone marrow in preneoplastic gammopathy. JCI Insight. 2019;5(11):e127807.
35. Krejcik J, Casneuf T, Nijhof IS, et al. Daratumumab depletes CD38+ immune regulatory cells, promotes T-cell expansion, and skews T-cell repertoire in multiple myeloma. Blood. 2016;128(3):384-394.
36. Cibrián D, Sánchez-Madrid F. CD69: from activation marker to metabolic gatekeeper. Eur J Immunology. 2017;47(6):946-953.
37. Glavey SV, Naba A, Manier S, et al. Proteomic characterization of human multiple myeloma bone marrow extracellular matrix. Leukemia. 2017;31(11):2426-2434.
38. Storti P, Marchica V, Airoldi I, et al. Galectin-1 suppression delineates a new strategy to inhibit myeloma-induced angiogenesis and tumoral growth in vivo. Leukemia. 2016;30(12):2351-2363.
39. Clemente T, Vieira NJ, Cerliani JP, et al. Proteomic and functional analysis identifies galectin-1 as a novel regulatory component of the cytotoxic granule machinery. Cell Death Dis. 2017;8(12):e3176.
40. Dhodapkar KM, Cohen AD, Kaushal A, et al. Changes in bone marrow tumor and immune cells correlate with durability of remissions following BCMA CAR T therapy in myeloma. Blood Cancer Discov. 2022;3(6):490-501.
41. Labiano S, Meléndez-Rodríguez F, Palazón A, et al. CD69 is a direct HIF-1α target gene in hypoxia as a mechanism enhancing expression on tumor-infiltrating T lymphocytes. Oncoimmunology. 2017;6(4):e1283468.
42. Doedens AL, Phan AT, Stradner MH, et al. Hypoxia-inducible factors enhance the effector responses of CD8(+) T cells to persistent antigen. Nat Immunol. 2013;14(11):1173-1182.
43. Xu Y, Chaudhury A, Zhang M, et al. Glycolysis determines dichotomous regulation of T cell subsets in hypoxia. J Clin Invest. 2016;126(7):2678-2688.